

**Supplementary Materials for**  
**“DNA replication studies of *N*-nitroso compound-induced *O*<sup>6</sup>-alkyl-2'-  
deoxyguanosine lesions in *Escherichia coli*”**

Pengcheng Wang<sup>1,2</sup>, Jiapeng Leng<sup>1</sup> and Yinsheng Wang<sup>1\*</sup>

<sup>1</sup>Department of Chemistry, University of California, Riverside, California 92521-0403, United States

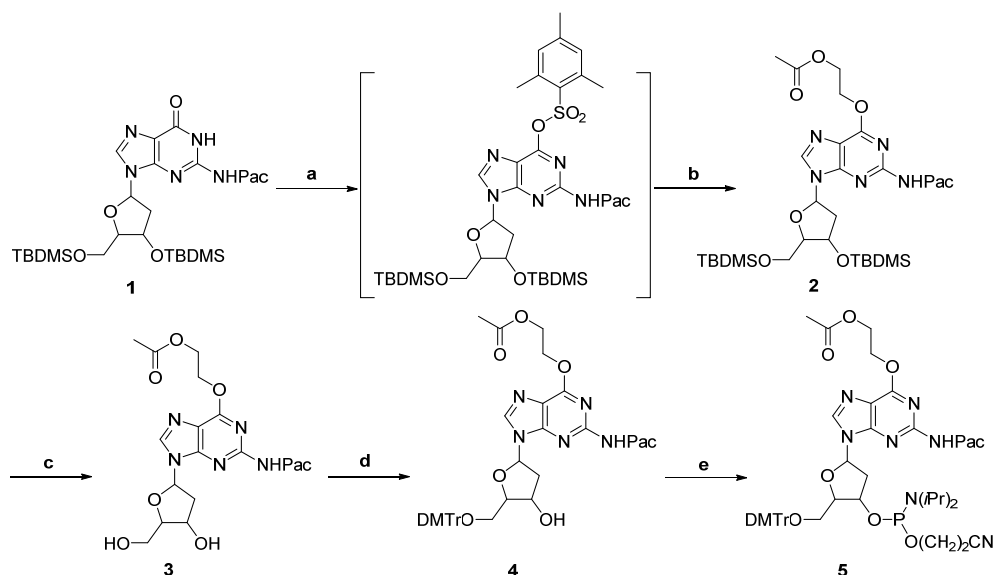
<sup>2</sup>Institute of Surface Analysis and Chemical Biology, University of Jinan, Jinan, Shandong 250022, China

\*To whom correspondence should be addressed: Tel. (951)827-2700; E-mail:

Yinsheng.Wang@ucr.edu

## Supplementary Materials and Methods:

### Scheme S1. Synthetic procedures for the phosphoramidite building block of $O^6$ -HOEt-dG\*



\*Reagents and conditions: a) 2-mesitylenesulfonyl chloride, DMAP, 40 min; b) *N*-methylpyrrolidine, 30 min; ethylene glycol monoacetate, DBU, 6 h; c) TBAF, THF, r.t., 1 h; d) DMTr-Cl, DMAP, pyridine, r.t., 10 h; e) 2-cyanoethyl-*N,N*-diisopropyl chlorophosphoramidite, DIEA,  $\text{CH}_2\text{Cl}_2$ , 1 h.

### Reaction yields, and NMR and mass spectrometric characterizations of the synthetic products:

**3',5'-*O*-Bis(*tert*-butyldimethylsilyl)-*N*<sup>2</sup>-(phenylacetyl)-*O*<sup>6</sup>-acetyloxyethoxyl-2'-deoxyguanosine (2).** Obtained as brownish solid (42% yield);  $^1\text{H}$  NMR (400 MHz,  $\text{CDCl}_3$ )  $\delta$  8.21 (s, 1H), 7.92 (s, 1H), 7.43 – 7.28 (m, 5H), 6.42 (t,  $J = 6.4$  Hz, 1H), 4.76 – 4.72 (m, 2H), 4.60 (dt,  $J = 5.8, 3.6$  Hz, 1H), 4.50 – 4.46 (m, 2H), 4.17 (s, 2H), 4.02 (dd,  $J = 6.7, 3.3$  Hz, 1H), 3.83 (ddd,  $J = 14.3, 11.3, 3.4$  Hz, 2H), 2.55 (dt,  $J = 12.7, 6.3$  Hz, 1H), 2.47 – 2.39 (m, 1H), 2.07 (s, 3H), 0.93 (s, 9H), 0.92 (s, 9H), 0.11 (s, 12H). HRMS (ESI) calcd for  $\text{C}_{34}\text{H}_{54}\text{N}_5\text{O}_7\text{Si}_2$   $[\text{M}+\text{H}]^+$  700.3556, found 700.3562.

***N*<sup>2</sup>-(phenylacetyl)-*O*<sup>6</sup>-acetyloxyethoxyl-2'-deoxyguanosine (3).** Obtained as yellowish film (56% yield);  $^1\text{H}$  NMR (400 MHz,  $\text{CDCl}_3$ )  $\delta$  8.20 (s, 1H), 8.16 (s, 1H), 7.43 – 7.28 (m, 5H), 6.34 (t,  $J = 6.7$  Hz, 1H), 5.32 (s, 1H), 4.93 – 4.88 (m, 1H), 4.75 – 4.69 (m, 2H), 4.48 – 4.42 (m, 2H), 4.17 – 4.12 (m, 1H), 4.01 – 3.81 (m, 4H), 3.36 – 3.28 (m, 1H), 2.92 (dt,  $J = 13.3, 6.6$  Hz, 1H),

2.47 – 2.39 (m, 1H), 2.05 (s, 3H). HRMS (ESI) calcd for C<sub>22</sub>H<sub>26</sub>N<sub>5</sub>O<sub>7</sub> [M+H]<sup>+</sup> 472.1827, found 472.1836.

**5'-O-(4,4'-dimethoxytrityl)-N<sup>2</sup>-(phenylacetyl)-O<sup>6</sup>-acetyloxyethoxyl-2'-deoxyguanosine (4).**

Obtained as yellowish foam (51% yield); <sup>1</sup>H NMR (400 MHz, CD<sub>3</sub>OD) δ 8.26 (s, 1H), 7.35 – 7.13 (m, 14H), 6.70 (dd, *J* = 17.3, 8.9 Hz, 4H), 6.46 (t, *J* = 6.5 Hz, 1H), 4.84 – 4.81 (m, 1H), 4.78 (dd, *J* = 5.8, 3.2 Hz, 2H), 4.52 – 4.48 (m, 2H), 4.15 – 4.10 (m, 1H), 3.86 (s, 2H), 3.75 (s, 3H), 3.74 (s, 3H), 3.45 (dd, *J* = 10.4, 6.4 Hz, 1H), 3.25 (dd, *J* = 10.4, 2.8 Hz, 1H), 3.06 – 2.97 (m, 1H), 2.54 – 2.45 (m, 1H), 2.03 (s, 3H). HRMS (ESI) calcd for C<sub>43</sub>H<sub>44</sub>N<sub>5</sub>O<sub>9</sub> [M+H]<sup>+</sup> 774.3134, found 774.3143.

**5:** <sup>31</sup>P NMR (120 MHz, CDCl<sub>3</sub>): δ 149.85, 149.79.

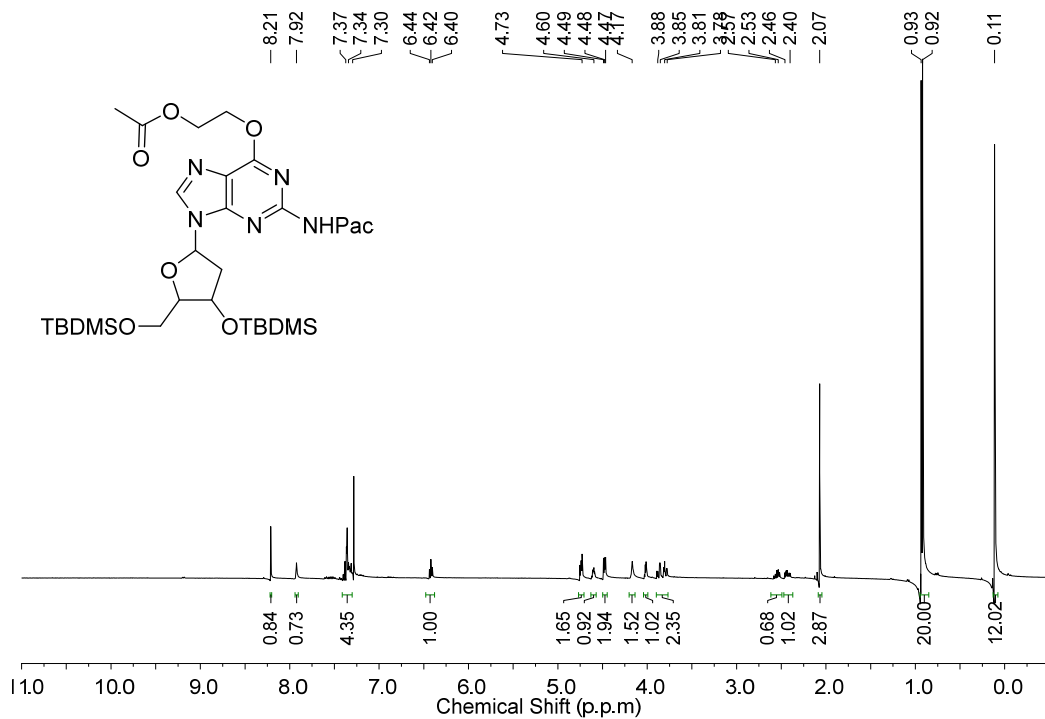


**Figure S1.** <sup>1</sup>H NMR spectrum of **2** (400 MHz, CDCl<sub>3</sub>, 25°C).

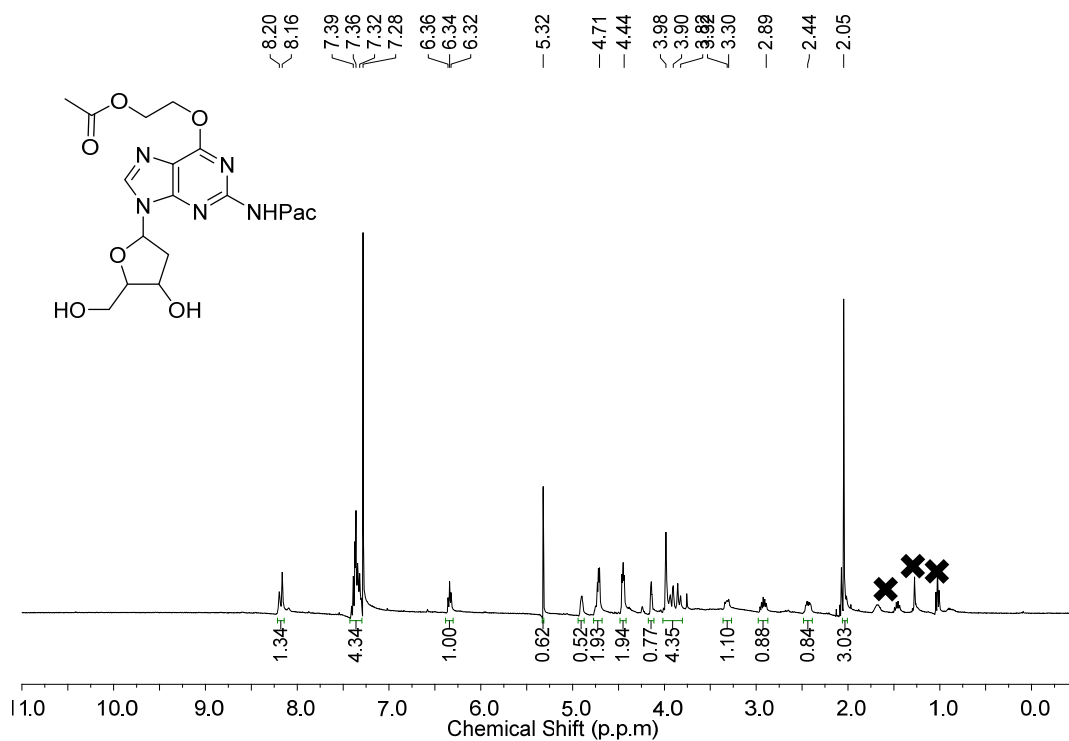


**Figure S2.** <sup>1</sup>H NMR spectrum of **3** (400 MHz, CDCl<sub>3</sub>, 25°C). 'X' indicates peaks from residual TBAF.

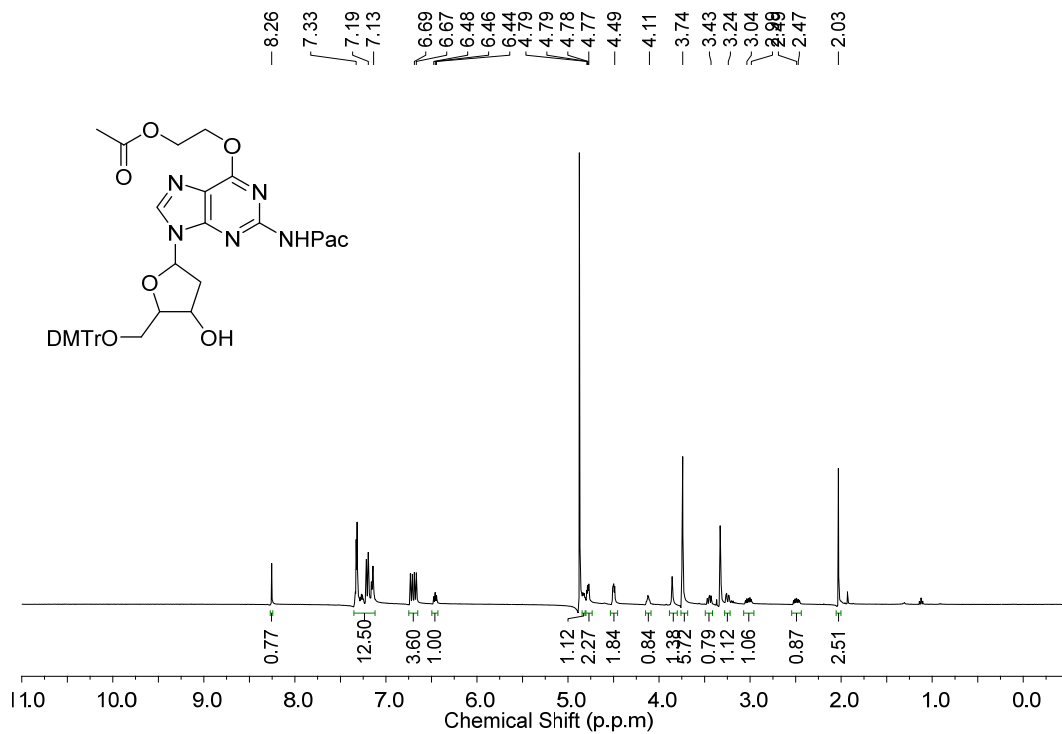


**Figure S3.**  $^1\text{H}$  NMR spectrum of **4** (400 MHz,  $\text{CD}_3\text{OD}$ ,  $25^\circ\text{C}$ ).

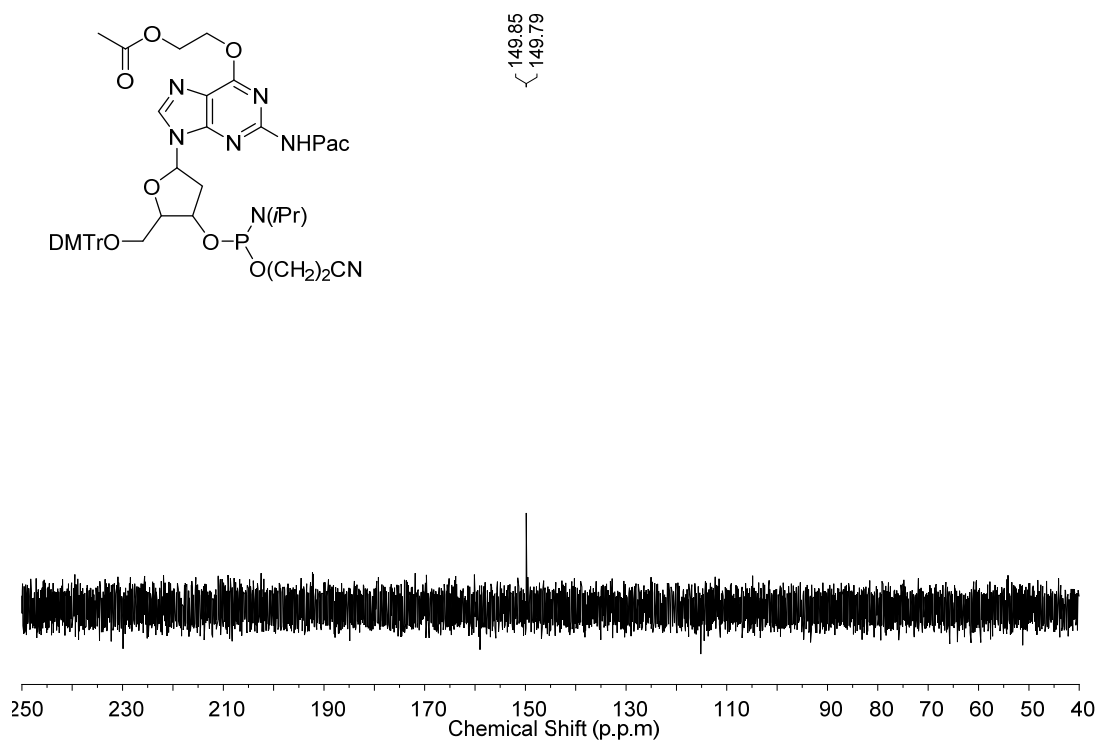


**Figure S4.**  $^{13}\text{C}$  NMR spectrum of **5** (80 MHz,  $\text{CDCl}_3$ ,  $25^\circ\text{C}$ ).

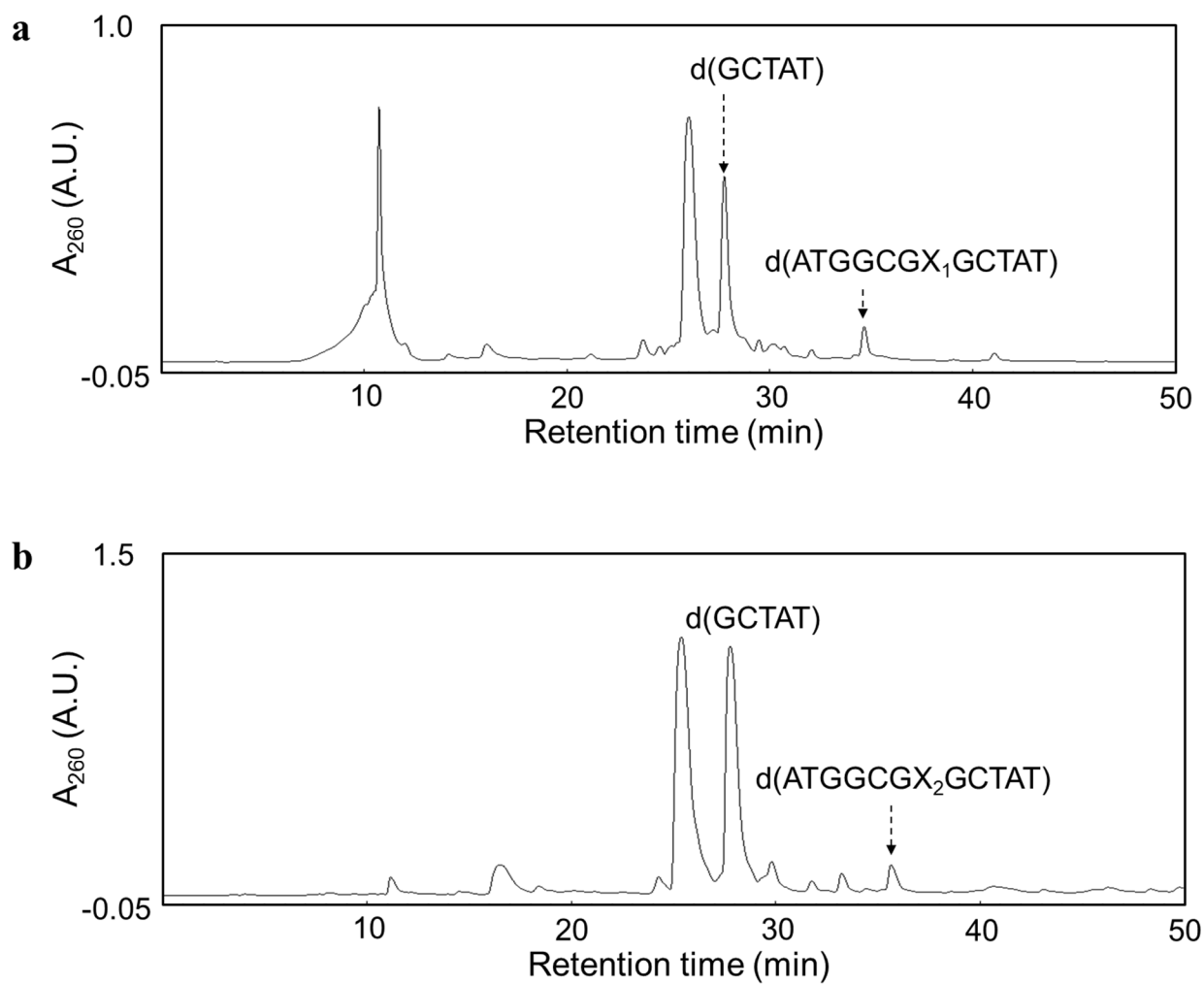


**Figure S5.** HPLC traces for the separation of the synthesized 12mer ODNs: (a)  $X_1 = O^6\text{-ACM-dG}$  and (b)  $X_2 = O^6\text{-HOEt-dG}$ .

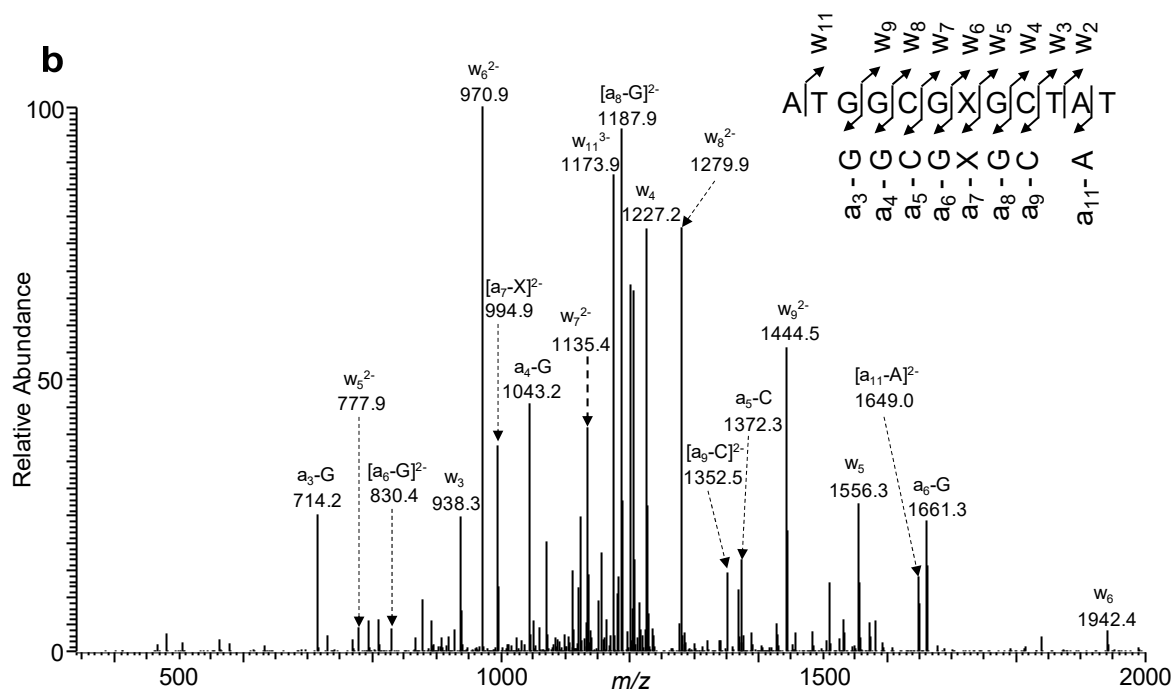
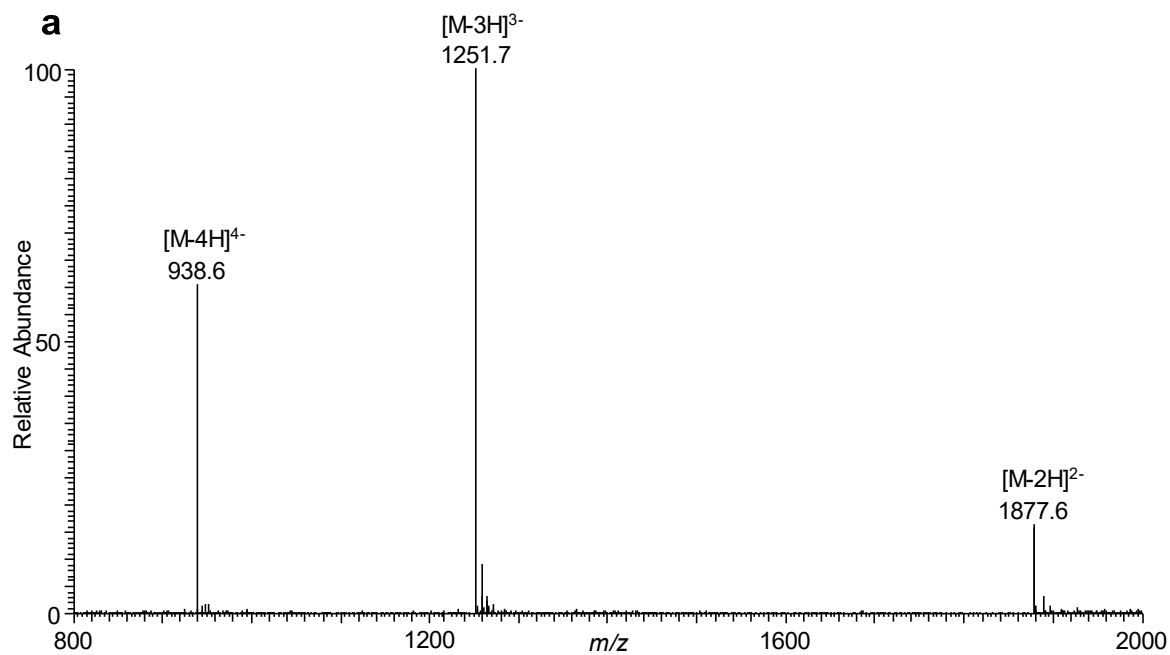


**Figure S6.** ESI-MS & MS/MS characterizations of d(ATGGCGXGCTAT), X=O<sup>6</sup>-ACM-dG. (a) Negative-ion ESI-MS; (b) the product-ion spectrum of the  $[M-3H]^{3-}$  ion ( $m/z$  1251.7).

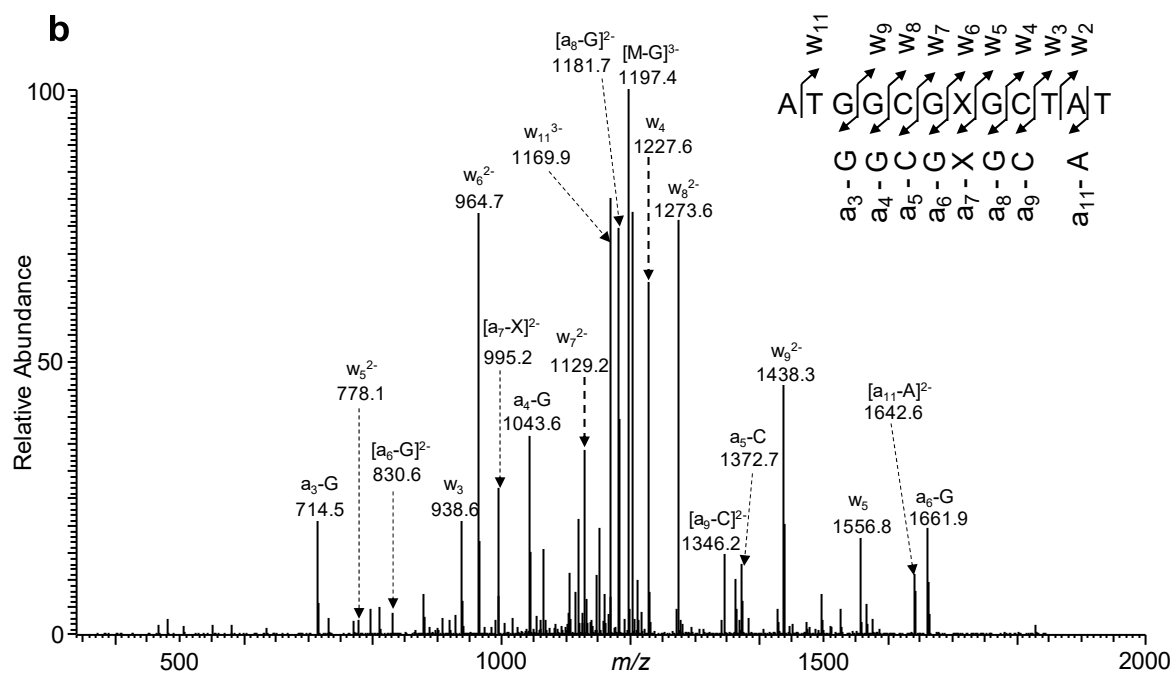
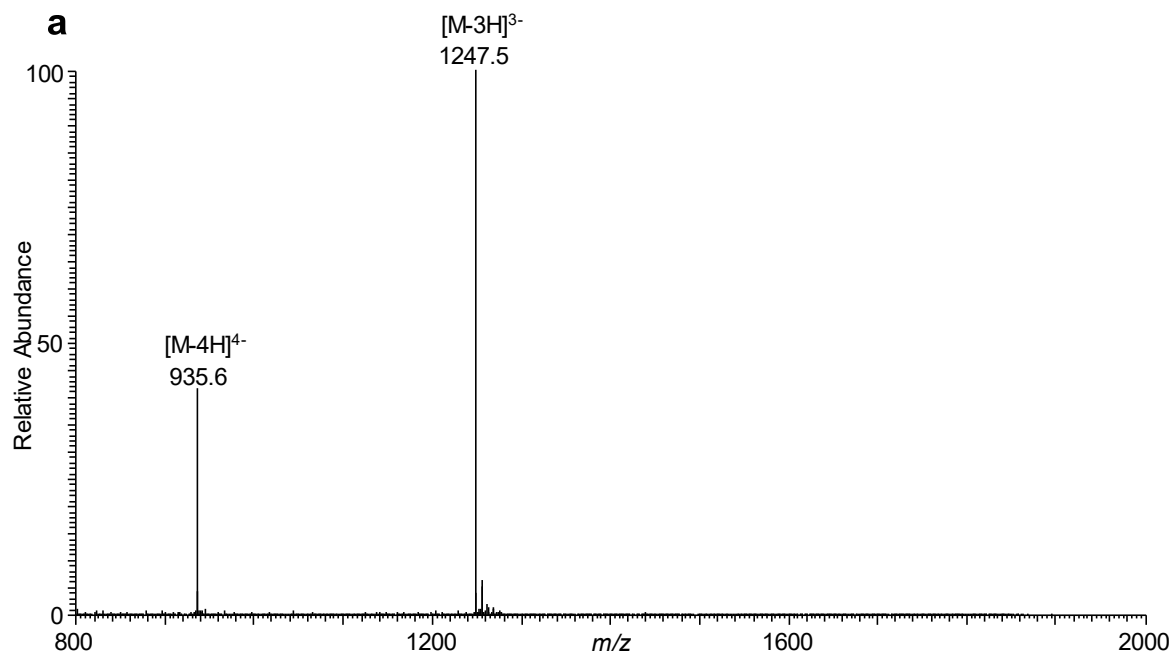


**Figure S7.** ESI-MS & MS/MS characterizations of d(ATGGCGXGCTAT), X=O<sup>6</sup>-HOEt-dG. (a) Negative-ion ESI-MS; (b) the product-ion spectrum of the  $[M-3H]^{3-}$  ion ( $m/z$  1247.5).



**a. Construction of the Lesion-containing genome:**

5'-GAAAGCTATGACCATGATTCAGTGAGTGGAAAGACATGGCGXGCTATAATTCACTGGCCGTCGTTTT-3'  
3'-CTTTCGATACTGGTACTAAGTCACTCACCTTC-3'      3'-CGATATTAAGTGACCGGCAGCAAAA-5'

**b. Construction of the competitor genome:**

5'-AGCTATGACCATGATTCAGTGAGTGGAAAGACATGGCGATAAGCTATAATTCACTGGCCGTCGTT-3'  
3'-TCGATACTGGTACTAAGTCACTCACCTTC-5'      3'-CGATATTAAGTGACCGGCAGCAA-5'

**Figure S8.** Schematic diagrams showing the constructions of the lesion-containing (a) and competitor (b) genomes. Displayed are the partial sequence of the linearized M13, the 22-mer lesion-containing or the 25-mer lesion-free competitor insert (shown in red), and the two scaffolds employed for the ligation reactions. The lesion site is underlined (X).

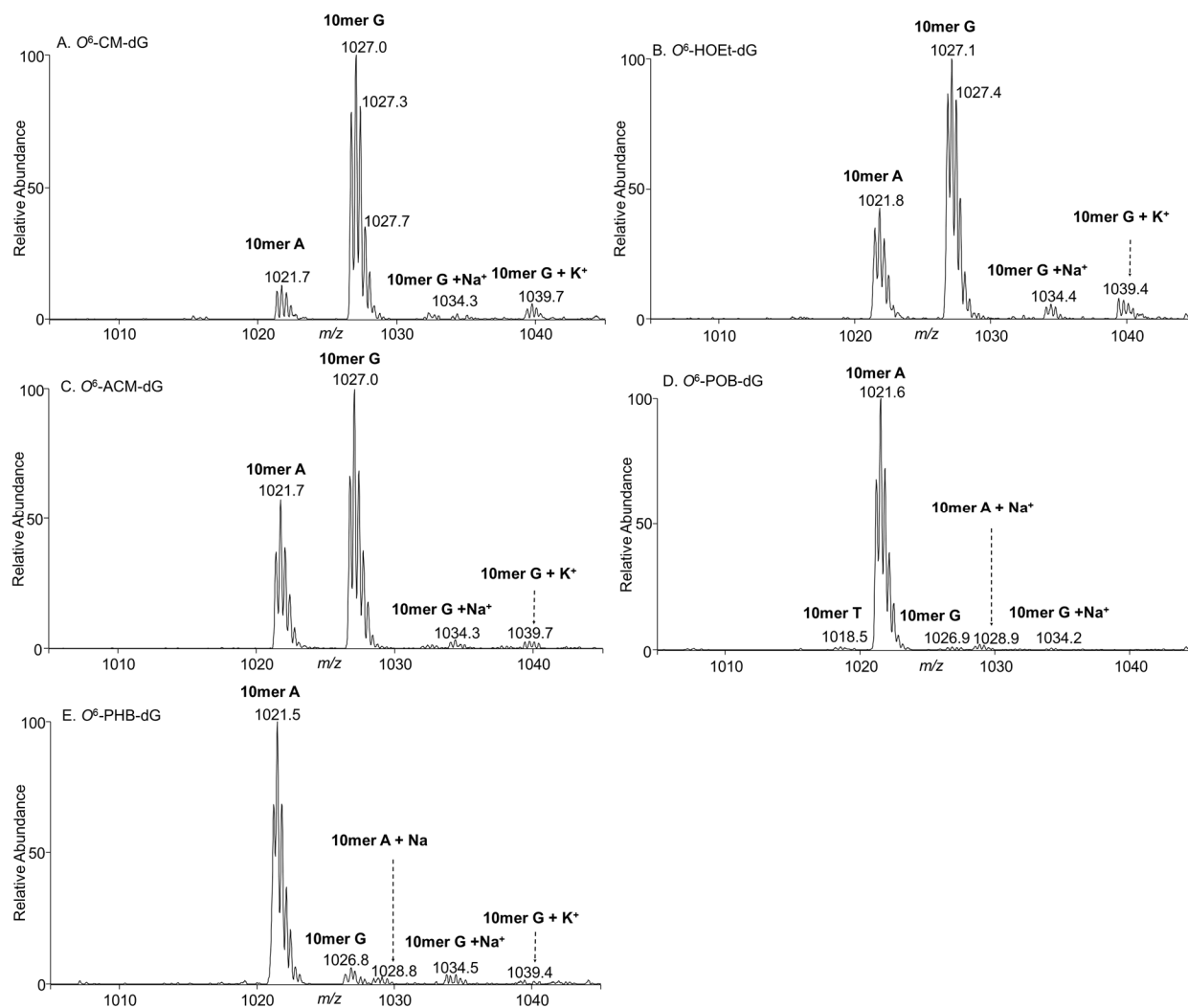


**Figure S9.** Higher-resolution “zoom” scan ESI-MS for monitoring the  $[M - 3H]^{3-}$  ions of the lesion-containing strand of the restriction fragments of the PCR products from the replication of: (A)  $O^6$ -CM-dG-, (B)  $O^6$ -HOEt-dG-, (C)  $O^6$ -ACM-dG-, (D)  $O^6$ -POB-dG-, and (E)  $O^6$ -PHB-dG-bearing single-stranded M13 genomes in SOS-induced wild-type AB1157 cells. The G→A and G→T mutation products were further confirmed by MS/MS analyses, and representative MS/MS results for  $O^6$ -POB-dG are shown in Figure S10.

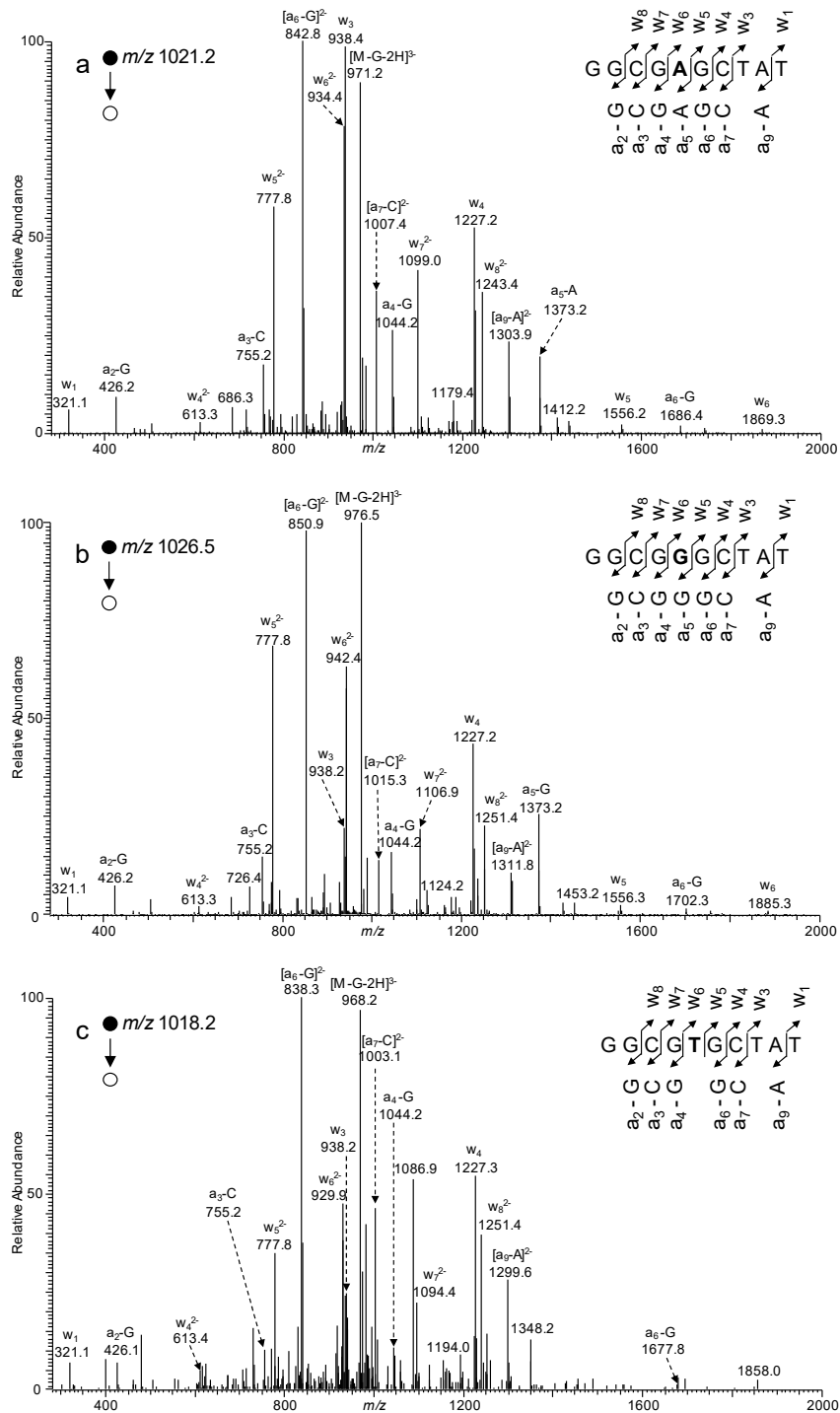
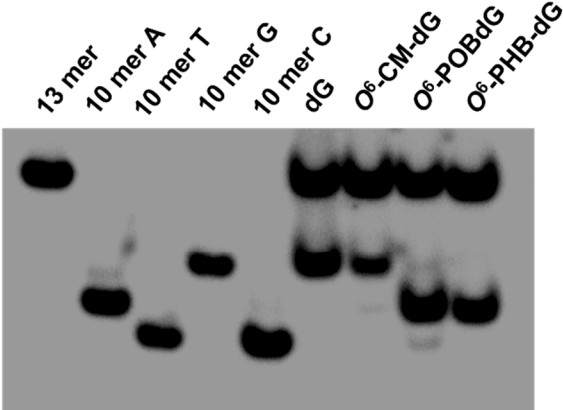
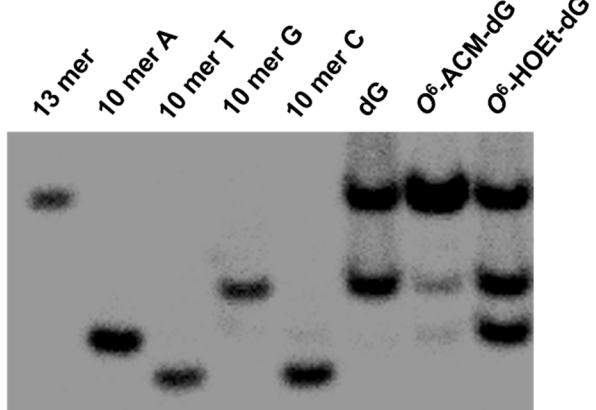


**Figure S10.** Representative LC-MS/MS data for the identification of (a) G→A mutation and (b) non-mutagenic product observed for the  $O^6$ -CM-dG, and (c) G→T mutation observed for  $O^6$ -POB-dG in SOS-induced wild-type (WT) AB1157 *E. coli* cells. Shown are the MS/MS for the  $[M - 3H]^3$  ions of (a) 10 mer A (G→A mutation), (b) 10 mer G (non-mutagenic product), and (c) 10 mer T (G→T mutation).

a WT



b WT



c WT-SOS

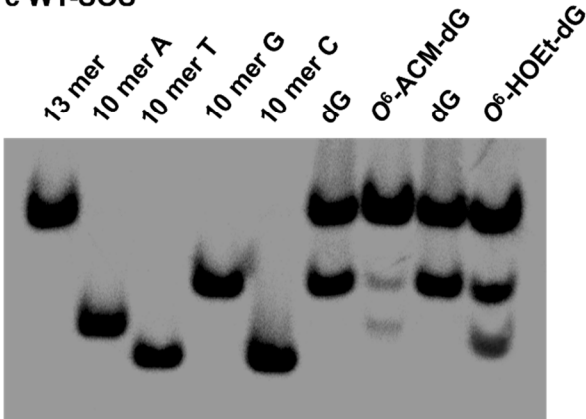


**Figure S11.** Native PAGE (30%) for monitoring the bypass efficiencies and mutation frequencies of (a)  $O^6$ -CM-dG,  $O^6$ -POB-dG, and  $O^6$ -PHB-dG in wild-type (WT) AB1157 *E. coli* cells; and  $O^6$ -ACM-dG, and  $O^6$ -HOEt-dG in (b) WT and (c) SOS-induced WT AB1157 *E. coli* cells. Gel image showing the 13-mer and 10-mer products released from the original lesion-situated strand of the PCR products of the progeny of the competitor genome (13-mer, i.e. 5'-GGCGATAAGCTAT-3') and the control or lesion-carrying genome (10-mer), where 10mer A, 10mer C, 10mer G, and 10mer T represent the [5'- $^{32}$ P]-labeled standard ODNs 5'-GGCGM<sub>M</sub>GCTAT-3', with 'M' being A, C, G, and T, respectively.

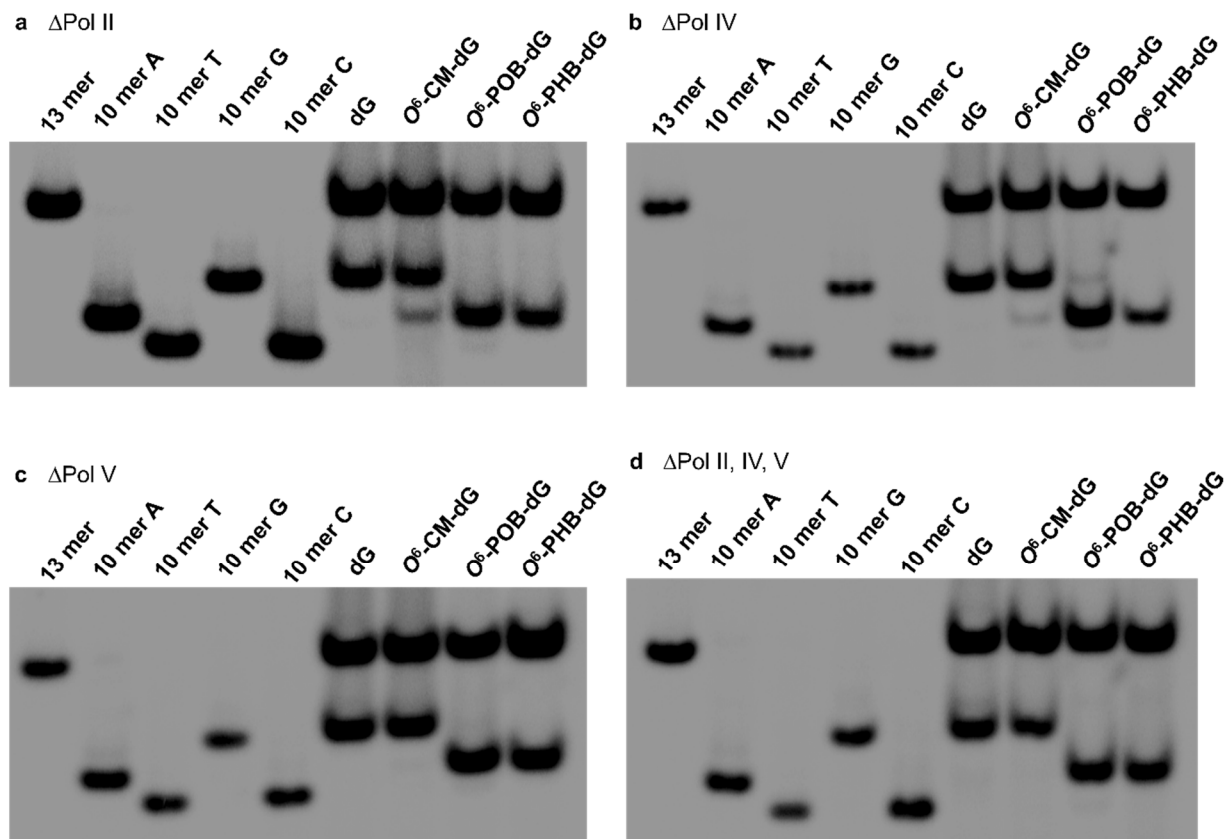


**Figure S12.** Native PAGE (30%) for monitoring the bypass efficiencies and mutation frequencies of  $O^6$ -CM-dG,  $O^6$ -POB-dG, and  $O^6$ -PHB-dG in SOS-induced AB1157 *E. coli* cells that are deficient in Pol II (a), Pol IV (b), Pol V (c), or all three translesion synthesis polymerases (d). Gel image showing the 13-mer and 10-mer products released from the original lesion-situated strand of the PCR products of the progeny of the competitor genome (13-mer, i.e. 5'-GGCGATAAGCTAT-3') and the control or lesion-carrying genome (10-mer), where 10mer A, 10mer C, 10mer G, and 10mer T represent the [5'-<sup>32</sup>P]-labeled standard ODNs 5'-GGCGMGCTAT-3', with 'M' being A, C, G, and T, respectively.

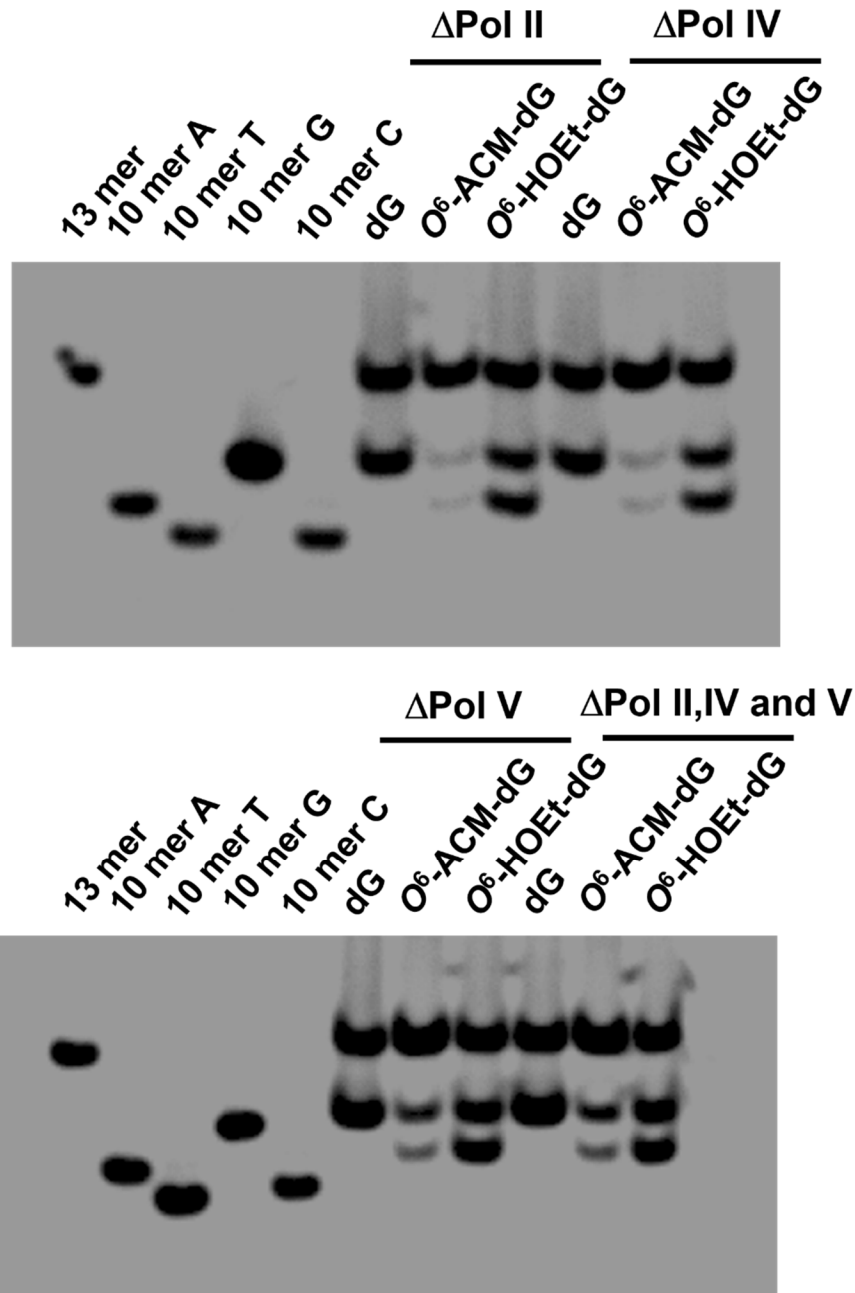


**Figure S13.** Native PAGE (30%) for monitoring the bypass efficiencies and mutation frequencies of  $O^6$ -ACM-dG, and  $O^6$ -HOEt-dG in SOS-induced AB1157 *E. coli* cells that are deficient in Pol II, Pol IV, Pol V, or all three translesion synthesis polymerases. Gel image showing the 13-mer and 10-mer products released from the original lesion-situated strand of the PCR products of the progeny of the competitor genome (13-mer, i.e. 5'-GGCGATAAGCTAT-3') and the control or lesion-carrying genome (10-mer), where 10mer A, 10mer C, 10mer G, and 10mer T represent the [5'- $^{32}$ P]-labeled standard ODNs 5'-GGCGMGCTAT-3', with 'M' being A, C, G, and T, respectively.

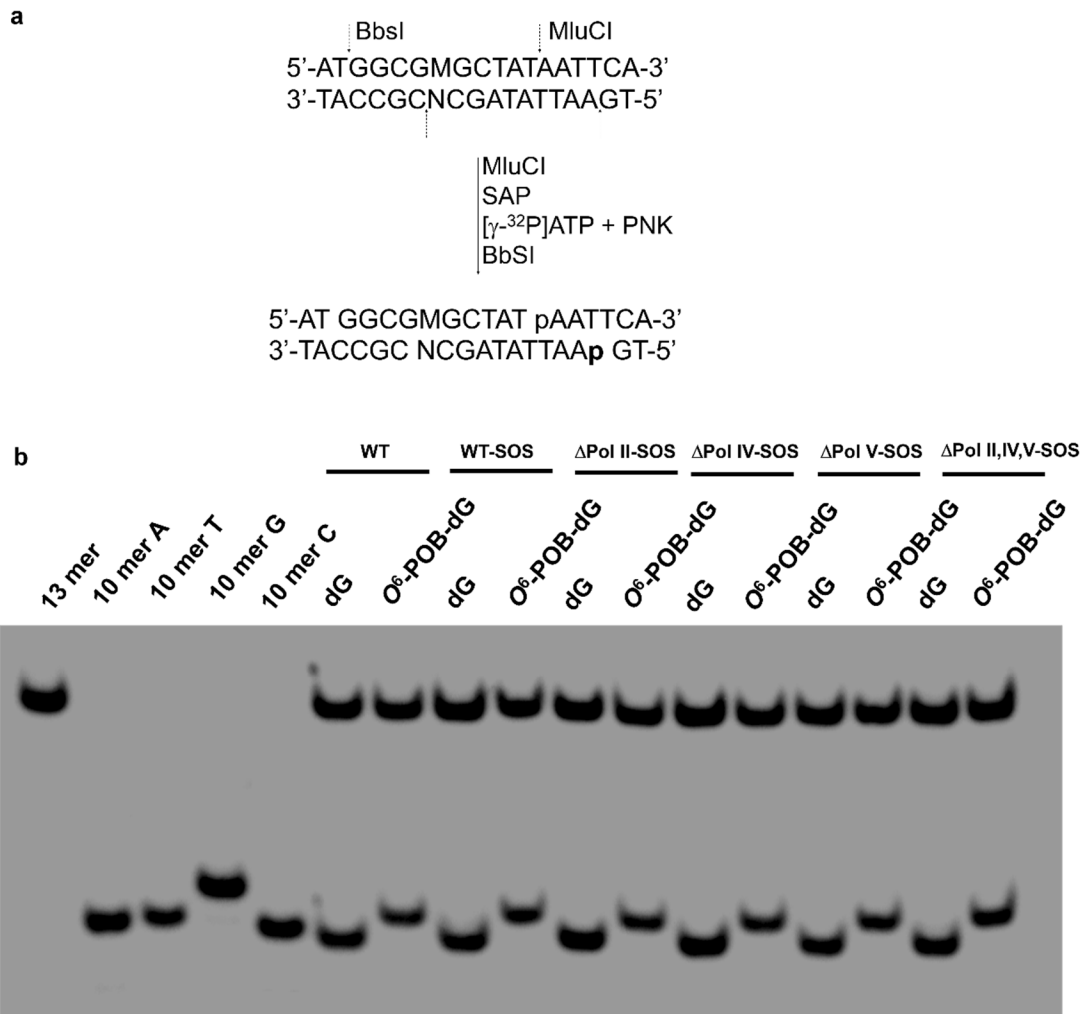


**Figure S14.** Native PAGE (30%) for monitoring the bypass efficiencies and mutation frequencies of *O*<sup>6</sup>-POB-dG lesions in AB1157 *E. coli* cells that are proficient or deficient in translesion synthesis polymerases. (A) Sequential restriction enzyme digestion and selective radio-labeling of the strand complementary to the strand initially containing the lesion. ‘SAP’ and ‘PNK’ designate shrimp alkaline phosphatase and T4 polynucleotide kinase, respectively. (B) Gel image showing the 13-mer and 10-mer radio-labeled restriction fragments released from the original lesion-containing strand of the PCR products of the progeny of the competitor genome and the control or lesion-carrying genome, where 10mer A, 10mer C, 10mer G, and 10mer T represent the [5’-<sup>32</sup>P]-labeled standard ODNs 5’-AATTATAGCN-3’, with ‘N’ being A, C, G, and T, respectively.